

Photocatalytic Degradation of Reactive Dyes in Effluents Employing Copper Doped Titanium Dioxide Nanocrystals and Direct Sunlight

P. DHARMARAJAN^a, A. SABASTIYAN^b, M. YOSUVA SUVAIKIN^{b*},
S. TITUS^b and C. MUTHUKUMAR^c

^aDepartment of Chemistry, Thanthai Hans Roever College, Perambalur - 621 212, India

^bDepartment of Chemistry, Urumu Dhanalakshmi College, Tiruchirappalli- 620019, India

^cDepartment of Chemistry, J.J.College of Arts and Science, Pudukkottai-622001, India
yosu77s@gmail.com

Received 3 March 2013 / Accepted 19 March 2013

Abstract: Nanosized photocatalyst samples of TiO₂ and Cu-doped TiO₂ were synthesized employing sol-gel method. The photocatalysts were characterized by powder XRD, SEM, EDAX and diffused reflectance spectral studies. Model effluents of reactive dyes were subjected to degradation employing the Cu-doped TiO₂ catalysts with direct sunlight irradiation and liberal aeration. The heterogeneous Advanced Oxidation Process (AOP) involves photolytic generation of very reactive hydroxyl radicals. The photocatalytic degradation activity of the nanocatalysts has been evaluated on the basis of Langmuir-Hinshelwood kinetic model. The effects of pH, concentration of H₂O₂ added, initial dye concentration and dosage of the catalyst have also been investigated. The degrees of degradation/mineralization of the organic dyes have also been estimated by measuring the CODs of the photocatalytically degraded dye solutions. The results show that the Cu-doped TiO₂ nanoparticles are very effective in degrading the dye pollutants.

Keywords: Cu-doped TiO₂ nanocrystals, Reactive dyes, Photocatalytic degradation, Advanced oxidation process, Hydroxyl radical, Chemical oxygen demand

Introduction

Environmental concerns have led to extensive research on the removal of organic compounds from industrial waste streams. Effluents from industries released into the environment cause many serious ecological problems. Textile industry is one generating large volumes of toxic waste water containing commercial dyes which are carcinogenic in nature. Heterogeneous advanced oxidation processes which involve hydroxyl radicals ([•]OH) are successfully used to degrade and mineralize organic pollutants^{1,2} present in waste waters into CO₂ and inorganic ions. Metal oxide semiconductors have been used as photocatalysts^{3,4} in the oxidation processes. TiO₂-mediated photocatalytic oxidation appears to be a promising technique for degradation of commercial dyes. Some metal ion doped TiO₂ is reported to have

better activity than the undoped TiO₂. In view of this, an attempt has been made to synthesize solar light active nanocrystals of Cu-doped TiO₂ for photocatalytic degradation of reactive dyes present in waste waters. TiO₂ is relatively cheap and non-toxic when compared to others. Physical modification of TiO₂ into nanoparticles has shown photocatalytic activity improvement to a large extent. Many researchers have synthesized visible light active anatase and rutile titania by doping transition metal ions such as Fe³⁺, Mo⁵⁺, Ru³⁺, V⁴⁺ and Rh⁴⁺ or nonmetals like N, C, F, P and S to narrow the band gap. Noble metal ion doping (Pt, Au, Pd Ag *etc.*) has also been reported to be effective for enhancement of TiO₂ photocatalysis⁵⁻⁹.

Reactive dyes are the single largest group of dyes used in textile industry. They have been chosen for the photocatalytic degradation studies over Cu-doped TiO₂ because it is very difficult to eliminate them by the usual biodegradation and sludge absorption techniques.

Experimental

Industrial grade reactive blue 4 (Na₂C₂₃H₁₂N₆O₈S₂Cl₂, λ_{max}=598 nm), reactive orange 30 (Na₄C₂₉H₁₃N₅O₁₃S₄Cl₂, λ_{max}=422 nm), reactive red 120 (Na₆C₄₄H₂₄N₁₄O₂₀S₆Cl₂, λ_{max}=515 nm) and reactive black 5 (Na₄C₂₆H₂₁N₅O₁₉S₆, λ_{max}=602 nm) supplied by Vexent Dyeans India Pvt Ltd., Mumbai were used for preparation of model effluents in distilled water, TiCl₄ (99.5% pure) supplied by Loba Chemie Pvt Ltd. was used for the preparation of TiO₂ photocatalyst. Other AR grade chemicals such as copper(II) acetate monohydrate, potassium dichromate, mercury(II) sulphate, silver(I) sulphate, ferrous ammonium sulphate (FAS) and ferroin indicator purchased from Qualigens were used as such.

An advanced Bruker AXS D8 diffractometer was used to obtain powder diffraction patterns of the photocatalyst samples. A scanning electron microscope JEOL Model JSM-6390 LV was used to analyze the surface morphology of the catalytic samples. Energy dispersed X-ray diffraction analysis (EDAX) was performed employing JEOL Model JED-2300 EDS analyzer. Diffuse reflectance spectral data were collected over the spectral range 300-800nm with a Perkin - Elmer Lambda 2D equipped with a 5 cm integrating sphere (Lab sphere). MgO was used as the reference material. Concentrations of the dye solutions were determined periodically by measuring absorbance at the respective λ_{max} values using an Elico-SL-171 visible spectrophotometer.

Preparation of copper-doped TiO₂ photocatalyst samples

TiO₂ and Cu-doped TiO₂ samples were synthesized using sol-gel method as reported elsewhere¹⁰. In a typical synthesis, 5 mL of TiCl₄ was added to 250 mL of ice cold distilled water with vigorous stirring over a period of half an hour. The hydrolysis reaction gave a colloidal solution indicating the formation of nano-sized TiO₂ particles. (The hydrolysis of TiCl₄ could be expressed as: TiCl₄ + 2H₂O → TiO₂ + 4H⁺ + 4Cl⁻) By adding ammonia solution, H⁺ ions were neutralized and flocculation of TiO₂ was effected. The precipitate was separated centrifugally and washed several times with distilled water.

In the process of copper doping, copper acetate in the respective molar ratio (Cu/Ti = 0.02, 0.04, 0.06, 0.08 and 0.1) was mixed with the TiO₂ gel and stirred with a magnetic stirrer for two hours for uniform dispersion. In each case the gel was dried at 100 °C to remove water and the dried solid was ground in an agate mortar and pressed into a ceramic crucible and finally calcined at 500 °C in a muffle furnace for completion of solid phase reactions.

Results and Discussion

Physicochemical Characterization of Photocatalytic Samples

X-Ray Diffraction Studies

The crystalline structures of calcined samples were determined by analyzing the powder XRD patterns recorded at room temperature with Cu K α radiation. Measurements were made in steps of 0.025° with count time of 2s in the range of 20-65°. The phases were identified with the aid of JCPDS files¹¹. From the full width at half maximum (FWHM) of the diffraction pattern the crystallite size was calculated in each case using Scherrer's equation¹².

$$\text{Crystallite size} = K\lambda / W \cos\theta$$

Where shape factor, $K = 0.89$ and $W =$ full width at half maximum peak. The powder XRD patterns of TiO₂ and Cu-doped TiO₂ are shown in Figure 1. The XRD patterns show that the major peaks are of anatase phase manifested by (101) planes at $2\theta = 25.5^\circ$. The (110) peak expected for rutile at $2\theta = 27.5^\circ$ is not present in any of the patterns indicating the absence of rutile phase. The peaks of anatase TiO₂ for the Cu-doped ones are broader than that of the undoped TiO₂. The average crystallite sizes calculated for different proportions of Cu using the Scherrer's equation from the (101) reflections of anatase are listed in Table 1. The mean crystallite size of the Cu-doped TiO₂ decreases as the proportion of Cu increases. Similar results of decrease of crystallite size by doping with several transition metals on TiO₂ are already reported. However the bulk crystalline structure remains virtually unchanged by the incorporation of dopant metals¹³.

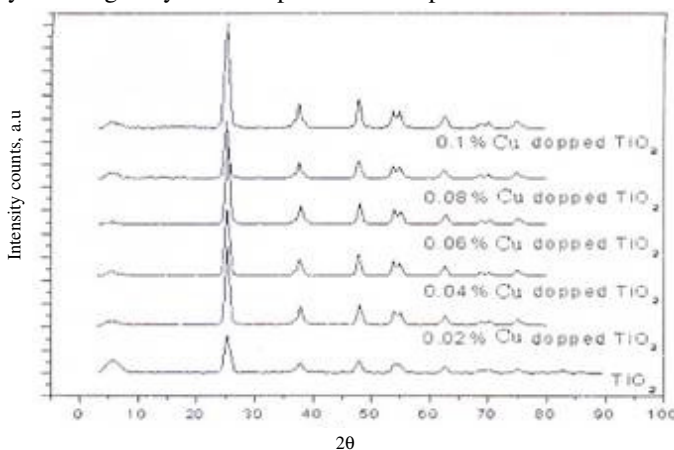


Figure 1. X-ray diffraction patterns of TiO₂ and Cu-doped TiO₂

Table 1. Effect of Cu doping on the crystallite Size of TiO₂

S.No	Photocatalyst	Full width half maximum for (1 0 1) diffraction (in degrees)	Crystallite size nm
1.	TiO ₂	0.551	44.9
2.	0.02% Cu-doped TiO ₂	0.611	40.5
3.	0.04% Cu-doped TiO ₂	0.671	36.9
4.	0.06% Cu-doped TiO ₂	0.673	36.8
5.	0.08% Cu-doped TiO ₂	0.700	35.3
6.	0.1 % Cu-doped TiO ₂	0.765	32.3

SEM and EDAX investigations on catalytic samples

In SEM photographs, both undoped TiO₂ and Cu-doped TiO₂ are found to exist as irregular agglomerates (Figure 2). But the Cu-doped TiO₂ samples are less agglomerated than the undoped TiO₂, indicating inhibition of agglomeration of TiO₂ nanoparticles by Cu^{II} ions. Lower level of agglomeration has been reported for the doping of Au on TiO₂¹⁴. The lower agglomeration of Cu-doped TiO₂ nanoparticles may be the inducement for a higher photocatalytic activity. The energy dispersive X-ray spectroscopic analyses of the Cu-doped TiO₂ also confirm the presence of Cu^{II} ions in the prepared photocatalysts.

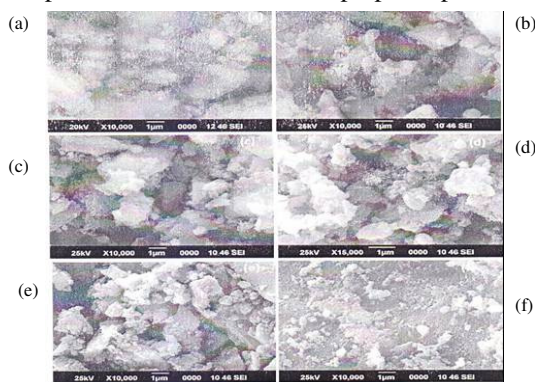


Figure 2. SEM images (a) TiO₂, (b) 0.02% Cu-doped TiO₂, (c) 0.04% Cu-doped TiO₂, (d) 0.06% Cu-doped TiO₂, (e) 0.08% Cu-doped TiO₂ and (f) 0.1% Cu-doped TiO₂

Diffuse reflectance spectral studies

Diffuse reflectance UV-visible spectra of TiO₂ and Cu-doped TiO₂ samples have been recorded to analyze the effect of doping with Cu^{II} ion on the absorption edge and optical band gap of TiO₂. The band gaps have been deduced from the Tauc plots. Tauc plot in each case is a plot of $[F(R)hv]^{1/2}$ versus photon energy (As representative cases the Tauc plots obtained for undoped TiO₂ and 0.02% Cu-doped TiO₂ are shown in Figures 3a and 3b). From the Tauc plots, the band gap energy values obtained are 3.19, 3.17, 3.16, 3.14, 3.12 and 3.11eV respectively for undoped, 0.02, 0.04, 0.06, 0.08 and 0.1% Cu-doped TiO₂ nanoparticles. This shows that the proportion of Cu dopant narrows down the band gap energy of the TiO₂.

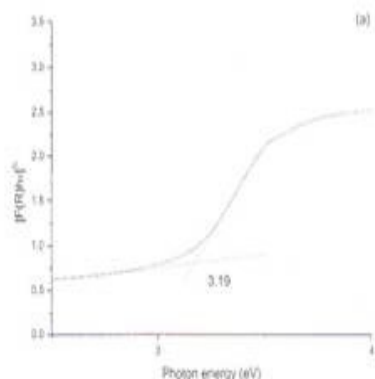


Figure 3a. Tauc plot for the diffuse reflectance data of TiO₂

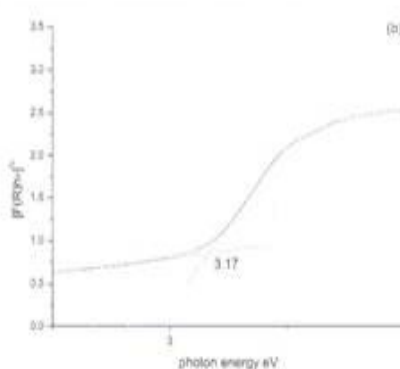


Figure 3b. Tauc plot for the diffuse reflectance data of 0.02% Cu-doped TiO₂

Studies on photocatalytic degradation of reactive dyes

All the dye degradation experiments were performed during clear sky days in summer period of 2012 under direct sunlight. In a typical experiment 50 mL of a dye solution was taken with 50 mg of the photocatalyst in a 250 mL glass beaker. The experimental set up was kept under direct sunlight with continuous aeration. The concentrations of the dye remaining (undegraded) were determined periodically by measuring the light absorbance at the λ_{\max} of the particular dye. In order to avoid variation in results due to fluctuation in the intensity of sunlight, a triplicate set of experiments was carried out simultaneously and the average of the results was noted.

To study the effect of pH of a dye solution on the photocatalytic degradation, the pH values of the dye solution were modified to different values (3, 5, 7, 9 and 12) by using 0.1 M HCl and 0.1 M NaOH solutions.

Photocatalytic degradation activity evaluation

The evaluation of activities of catalysts with reference to reactive blue 4 is discussed in detail. The degradation of reactive blue 4 as a function time is shown in Figure 4a. Analysis of the curves was carried out with the Langmuir - Hinshelwood kinetic model:

$$r = kKC/(1+KC),$$

Where r is the specific degradation reaction rate of the dye ($\text{mg L}^{-1}\text{min}^{-1}$), C is the concentration of the dye (mgL^{-1}), k is the rate constant (s^{-1}) and K is the dye adsorption constant. When C is small the above equation is simplified into an apparent first order rate equation¹⁵.

$$-dc/dt = r = kKC = k_{\text{app}}C$$

This equation on integration gives $-\ln C/C_0 = k_{\text{app}} t$ where C_0 is the initial concentration of the dye, C is the concentration of the dye after t minutes of illumination. The data obtained fit well into the pseudo first order rate equation as shown in Figure 4b and the rate constant values are listed in Table 2. The results show that rate constant values for the degradation of reactive blue 4 increase with the concentration of the Cu dopant upto 0.04% and further increase of Cu doping decreases the rate constants. It indicates that 0.04% Cu doping is optimum for maximum activity of TiO_2 . The dopant sites act as recombination centres when the concentration exceeds the optimum level¹⁶, which leads to reduction in the photocatalytic activity

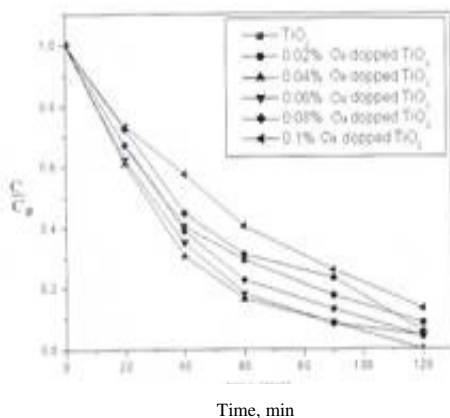


Figure 4a. Concentration Vs. time plots for photocatalytic degradation of reactive blue 4

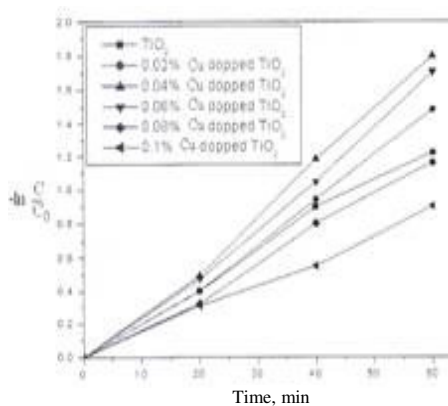


Figure 4b. Pseudo first order kinetic plots for the degradation of reactive blue 4

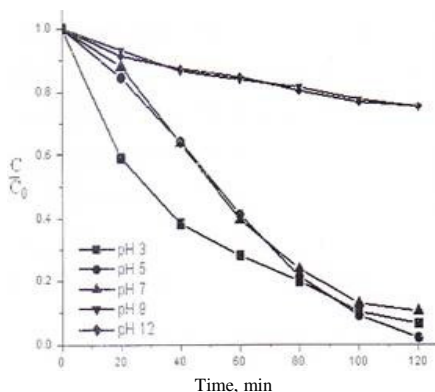
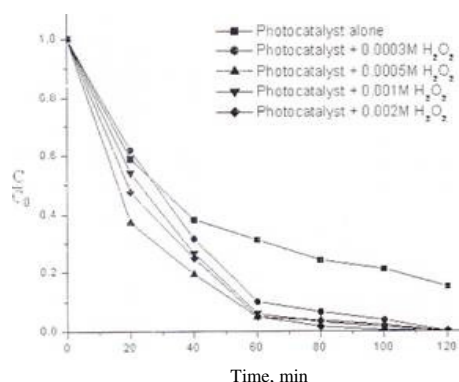
Table 2. Pseudo first order rate constant values for degradation of reactive blue 4 over TiO₂ and Cu-doped TiO₂

Photocatalyst	Pseudo first order rate constant, k	R ²
TiO ₂	0.0268	0.996
0.02% Cu-doped TiO ₂	0.0347	0.995
0.04% Cu-doped TiO ₂	0.03689	0.997
0.06% Cu-doped TiO ₂	0.0310	0.995
0.08% Cu-doped TiO ₂	0.0288	0.993
0.1 % Cu-doped TiO ₂	0.0239	0.992

Effect of pH of the dye solution on photocatalytic activity

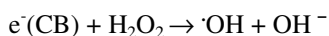
The variation of solution pH changes the surface of the TiO₂ nanoparticles and shifts the potential of the catalytic reaction. Under acidic pH surface of titania is protonated and remains positively charged. Under alkaline condition the surface is deprotonated and remains negatively charged. Under acidic conditions, the positively charged catalytic surface could adsorb strongly the dye anions. This facilitates the hydroxyl radicals to attack the dye molecules more easily¹⁷. But in alkaline condition adsorption of dye on the TiO₂ surface decreases because of the repulsion between negatively charged catalytic surface and dye anions resulting in a decrease of photocatalytic degradation rate¹⁸. Thus the effect of change of pH on the photocatalytic degradation of Reactive Blue 4 is shown in Figure 5.

The photocatalytic degradation of reactive blue 4 has been studied at different H₂O₂ concentrations and the results are summarized in Figure 6. The degradation of the dye increases with increasing H₂O₂ concentration up to 0.001 M, the optimum load¹⁹.

**Figure 5.** Effect of pH on photocatalytic degradation of reactive blue 4 on 0.1% Cu-doped TiO₂**Figure 6.** Effect of concentration of H₂O₂ on photocatalytic degradation of reactive blue 4 on Cu-doped TiO₂

Effect of concentration of hydrogen peroxide

Oxygen is the primary acceptor of the conduction band (CB) electron with the formation of superoxide radical anion. H₂O₂ can compensate for the O₂ lack and play a role as an external electron scavenger. It can trap the photogenerated CB electron, thus inhibiting the electron-hole recombination and producing hydroxyl radicals as shown here



H_2O_2 may also be photolysed to produce OH^\cdot radical directly ($\text{H}_2\text{O}_2 \rightarrow 2 \cdot\text{OH}$). But H_2O_2 has extremely low absorption of solarlight. Hence oxidative degradation of the dye beyond optimum load of H_2O_2 is insignificant. The inhibition of degradation of the dye beyond optimum load of H_2O_2 may be due to the hydroxyl radical scavenging effect of H_2O_2 . The hydroperoxy radicals formed are much less reactive and do not involve in oxidative degradation of the dye.

Effect of dye concentration

The influence of initial concentration of dye solution on degradation efficiency with time is shown in Figure 7. Increasing concentration of the dye solution decreases the percentage of degradation of the dye. As initial concentration increases more dye molecules are adsorbed on TiO_2 surface thereby reducing the generation of hydroxyl radicals. As the formation of $\cdot\text{OH}$ radicals decreases the percentage degradation of the dye also decreases²⁰⁻²².

Effect of dosage of the catalysts

The dye degradation increases with increasing catalyst concentration from 0.5 gL^{-1} to 1 gL^{-1} . This is characteristic of the heterogeneous photocatalysis. The increase in catalyst amount actually increases the number of active sites on the catalytic surface causing an increase in the number of $\cdot\text{OH}$ radicals which really take part in degradation of dye molecules. There is no significant improvement in the rate of degradation of dye when the dosage is above 1 gL^{-1} . Beyond 1 gL^{-1} level the solution becomes turbid and a portion of light radiation is blocked²³. The results are shown in Figure 8.

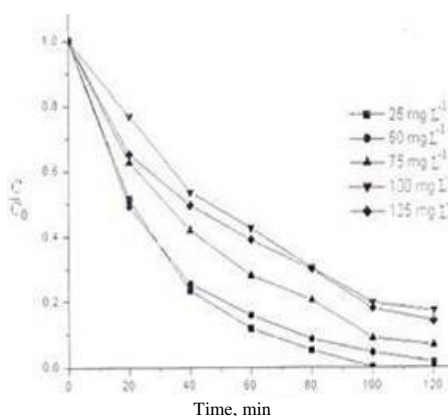


Figure 7. Effect of concentration of reactive blue 4 on photocatalytic degradation by Cu-doped TiO_2

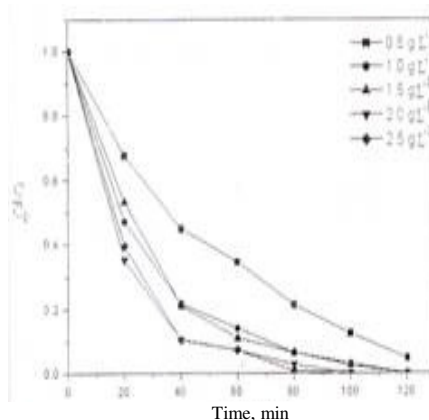


Figure 8. Effect of dosage of Cu-doped TiO_2 on photocatalytic degradation of reactive blue 4

Photocatalytic degradations of other reactive dyes

The degradations of three more reactive dyes *viz.* Reactive red 120, reactive black 5 and reactive orange 30 were also studied. The initial concentration of the dye solution used was 50 mgL^{-1} and pH was 5. The concentrations of the photocatalyst and oxidant were 1 gL^{-1} and 0.01 M respectively. The results show that the degradation of all the three dyes on Cu-doped TiO_2 is faster than that on TiO_2 . The Cu-doped TiO_2 completely degraded all the three dyes (50 mgL^{-1}) in 120 minutes with solar light irradiation.

Chemical oxygen demand (COD) analysis

COD is widely measured to estimate the level of organic load in the waste water and also to estimate the degree of degradation/ mineralization of organic pollutants in waste water treatments. The organic load is measured in terms of total quantity oxygen required to oxidize it into CO₂ and water. To measure COD, to 20 mL of the degraded dye solution taken in a 250 mL round bottomed flask, 0.4 g of Hg SO₄ and 10 mL of 0.25N K₂Cr₂O₇ solution were added and mixed well. Then 30 mL of H₂SO₄, AgSO₄ reagent (0.5 g AgSO₄ in 30 mL of Conc.H₂SO₄) was added slowly with constant stirring and the mixture refluxed for 2 h. The mixture was cooled, diluted to 150 mL with distilled water and titrated against 0.25 N ferrous ammonium sulphate (FAS) solution using ferroin indicator. COD was calculated using the equation:

$$\text{COD (in mg/L)} = (V_2 - V_1) \times N \times 8 / X$$

Where V₁ and V₂ are the volumes of FAS solution consumed by the blank and test sample respectively, N is the normality of FAS solution and X is the volume of sample taken for analysis. Table 3 gives the percentages of reduction in COD of 50 mgL⁻¹ solutions of dyes on photocatalytic treatment over Cu-doped TiO₂ for two hours at pH 5 with catalyst dosage of 1 gL⁻¹ and H₂O₂ concentration of 0.001 M. The reduction in COD values of the treated dye solutions indicates that the mineralization of dyes takes place in a slower rate when compared to the degradation of the dyes.

Table 3. COD removal values for the dye solutions (50 mgL⁻¹)

Dye	Time of irradiation, hours	% of Degradation	% of Reduction in COD
Reactive blue 4	2	100	67.2
Reactive red 120	2	100	64.1
Reactive black 5	2	100	70.5
Reactive orange 30	2	100	76.3

Conclusion

The Cu-doped TiO₂ nanocrystals prepared by sol-gel method show an absorption threshold extended into the visible region. Cu-doped TiO₂ samples have higher activity in sun light than the undoped TiO₂. Addition of 1 mM of H₂O₂ increases the rate of degradation of the dyes. But concentrations beyond 1 mM do not increase the degradation much due to formation of less reactive peroxy radical. Photocatalyst dosage of 1 gL⁻¹ was optimum and acidic pH was more suitable for photocatalytic degradation of anionic dyes. The extent of photocatalytic degradation of the dyes has also been studied by COD measurement.

Acknowledgement

The authors express their thanks to the authorities of Urumu Dhanalakshmi College for extending their facilities. They also thank the SAIF IIT Chennai for extending their instrumentation facilities for physical measurements.

References

1. Huang C P, Dong C and Tang Z, *Waste Management*, 1993, **13**(5-7), 361-377.
2. Andreozzi R, Caprio V, Insola A and Martota R, *Cat Today*, 1999, **53**(1), 51-59.
3. Lasa H, Serrano B and Salaiques M, *Photocatalytic Reaction Engineering*; Springer: New York, 2005.

4. Brijesh Pare, Vijendra Singh and Jonnalagadda S B, *Indian J Chem.*, 2011, **50A**, 1061-1065.
5. Zhang Z, Wang C, Zhakaria R and Ying Y, *J Phys Chem B*, 1998, **102(52)**, 10871-1078.
6. Zhu J, Deng Z, Chen F, Zhang J, Chen H, Anpo M, Huang J and Zhang L, *Appl Catal B: Environ.*, 2006, **62**, 329-335.
7. Zhu J, Zheng W, He B, Jinlong Zhang and Anpo M, *J Mol Catal A: Chem.*, 2004, **216(1)**, 35-43.
8. Di Paola A, Marci G, Palmisano L, Schiavello M, Uosaki K, Ikeda S and Ohtani B, *J Phys Chem B*, 2002, **106(3)**, 637-645.
9. Nagaveni K, Hedge M S and Madras G, *J Phys Chem B*, 2004, **108(52)**, 20204-20212.
10. Xiangxin Yang, Chundi Cao, Larry Ericken, Kath Hohn, Ronardo Maghirang and Kenneth Klabunde, *Appl Catal B: Environ.*, 2009, **91(3-4)**, 657-662.
11. Praserttham P, Phungphadung J and Tanakulrungsank W, *Mater Res Innovations*, 2003, **7(2)**, 118-123.
12. Clark R J H, *J Chem Education*, 1964, **41(9)**, 488.
13. Murdoch M, Waterhouse G I N, Nadeem M A, Metson J B, Keane M A, Howe R F, Llorca J and Idriss H, *Nature Chem.*, 2011, **3(6)**, 489-492.
14. Mohamed M M and Al-Esaimi M M, *J Molecular Catal A: Chem.*, 2006, **255(1-2)**, 53-61.
15. Zhao W, Fu W, Yang H, Tian C, Li M, Ding J, Zhang W, Zhou Z, Zhao H and Li Y, *Nano-Micro Lett.*, 2011, **3(1)**, 20-24.
16. Sauer T, Cesconeto Neto G, Jose H J and Moreiral R F P M, *J Photochem Photobio A: Chem.*, 2002, **149(1-3)**, 147-154.
17. Wang Y and Hong C-S, *Water Res.*, 1999, **33(9)**, 2031-2036.
18. Malato S, Blanco J, Richter C, Braun B and Maldonado M I, *Appl Catal B: Environ.*, 1998, **17(4)**, 347-356.
19. Parra S, Stanca S E, Guasaquillo I and Thampi K R, *Appl Catalysis B: Environ.*, 2004, **51(2)**, 107-116.
20. Regina de Fatima P M M, Ticiane P S, Leonardo C, Eduardo H, *J Appl Electrochem.*, 2005, **35(7-8)**, 821-829.
21. Daneswar N, Salari D and Khatee A R, *J Photochem Photobio A: Chem.*, 2003, **157(1)**, 111-116.
22. Wang C C, Lee C K, Lyu M D and Juang L C, *Dyes and Pigments*, 2008, **76(3)**, 817-824.
23. Macedo L C, Zaia D A M, Moorie G J and De Satana H, *J Photochem Photobio A: Chem.*, 2007, **185(1)**, 86-93.